Water Permeability of Clay Sediment — Theory of Seepage Consolidation

A theory of seepage consolidation is described which uses the (non-seepage) sedimentation data to predict the water permeability of the sediment when seepage through a pervious bottom takes place. Theoretically, the infiltration resistance of sediment under seepage consolidation is a function of time, weight of solid per unit area, initial solid concentration, dynamic pressure drop across the system, and the characteristics of the sediment including the correlation between the permeability and the solid fraction, the correlation between the compressive stress of solid and solid fraction, and the tortuosity or axial ratio of the particles. In this article, the correlations mentioned above were obtained from batch sedimentation experiments. The dynamic pressure drop, the weight of solid per area, and the initial solid concentration are independent variables. When the axial ratio is 25, the theory predicts from numerical analysis an infiltration resistance–time curve and a seepage flow rate–time curve which match the experimental curves of a kaolinite system fairly well within the first 5 min. After that, deviations occur which are believed to be due to the wash-in mechanism in the real system.

INTRODUCTION

Particle settling is an important and ubiquitous phenomenon. Settling is called sedimentation in systems with low or intermediate particle content and consolidation when the system has a high solid content. Sedimentation and consolidation have been studied extensively in chemical engineering for solid-liquid separation, and in civil engineering for the construction of foundations, for example.

From the viewpoint of agriculture and soil science, the settling of particles in a soil matrix is critical because settling leads to the compaction of soil particles. The compaction determines water permeability, water sorption capacity and the soil aeration rate. Needless to say these are important factors in soil

ecology. Soil particles, particularly fine clays, are suspended in rain water when soil aggregates break down upon impact with rain drops. When rain water begins to seep into the soil matrix, clay particles may plug the pores of the soil matrix. Soon a thin layer of sediment forms due to the gravitational force acting on particles and the capillary suction forces from the soil underneath. Upon drying, the thin layer of sediment becomes even more dense due to the effect of surface tension. The entire process results in crust formation which is detrimental to the growth of plants. Since sediment is the precursor to crust formation, it is essential to understand the soil sedimentation and consolidation, and the effects of these on the seepage rate of rain water.

The early consolidation theory was developed by Terzaghi and Peck (1948) in their study of soil mechanics. Since then, many modifying theories and mathematical treatments have been reported in the literature, e.g., by McNabb (1960), Schiffman and Gibson (1964), Mikasa (1965), Raymond (1969), and Gibson et al. (1967, 1981). Experimentally, the effect of compaction on water permeability has been studied by Ruth (1946) and Tiller (1960) using compression-permeability cells.

Yagi and Yamazake (1960) applied the theory of consolidation to the process of sedimentation by assuming that the coefficient of consolidation was constant. Shirato et al. (1970) examined the settling of thick slurries and found that the settling process could be well analyzed from the viewpoint of the consolidation mechanism with variable consolidation coefficients. They derived a partial differential equation in which the gradient of the excess pore water pressure is related to the time-rate of the pressure. The coefficients of consolidation were obtained experimentally.

Shirato's treatment is very useful for studying systems with low compressive pressure, because the compression-permeability characteristics required in the analysis of these systems can be obtained easily from batch sedimentation experiments. Nevertheless, the mathematical treatment by Shirato et al. (1970) was limited to systems with an impervious bottom. Sedimentation in soil matrix, however, occurs with seepage from the bottom. It is highly desirable if one could use the sedimentation results to predict the consolidation behavior when seepage through a pervious bottom takes place. Therefore, in this article a theory is derived to treat particles settling in systems with the seepage of eluant from the bottom.

THEORY

Darcy's equation relates the excess pore water pressure, p, across a differential volume of porous solid, dw, to the relative velocity of flow according to

$$\epsilon(v_L - v_S) = -k\,\partial p/\partial w \tag{1}$$

where ϵ is the void fraction, and v_L and v_S are the velocities of liquid and solid, respectively, relative to the datum plane (see also Appendix II).

When the seepage flux is zero, i.e., $v_L=0$, the excess pore water pressure is simply the driving force per unit area for the flow opposite to the settling particles. In the case of $v_L>0$, the excess pore water pressure now is regarded as the sum of two pressures, p_u and p_d, where p_d is responsible for the downward flow vector, v_L, and p_u responsible for the upward flow vector, $-v_S$. Therefore:

$$\epsilon(v_L-v_S)=-k\,\partial(p_d+p_u)/\partial w \tag{2}$$

and by definition:

$$\epsilon v_L=-k\,\partial p_d/\partial w \tag{3a}$$

$$\epsilon v_S=-k\,\partial p_u/\partial w \tag{3b}$$

Because ϵv_L is invariant with respect to w, the pressure drop of p_d across a layer of sediment is proportional to its resistivity, $1/k$. From this relationship, it can be understood that p_d is the same entity as the dynamic pressure. Therefore, the dynamic pressure drop across the region from top to layer w is:

$$\Delta P(w)=\int_0^w(\epsilon v_L/k)\mathrm{d}w=v_F R(w) \tag{4}$$

where $R(w)$ is the resistance, and v_F is the eluant flux (at the point where $\epsilon=1$). The total resistance of the entire sediment is $R(w_0)$. Due to the friction when liquid seeps, the solid at layer w of the sediment sustains a differential stress proportional to the dynamic pressure drop multiplied by the void fraction and a tortuosity factor, τ (see Appendix I). Therefore, the cumulative stress over the layer w is obtained as follows.

$$p_e(w)=\int_0^w(\epsilon/\tau^2)\mathrm{d}p_d \tag{5}$$

where p_d at the layer w is related to the resistance $R(w)$ according to:

$$p_d(w)=p_d(w_0)R(w)/R(w_0) \tag{6}$$

Because p_e is the stress on the solid due to the seepage of liquid, it is called the seepage pressure.

The basic differential equation relating the gradient of velocity, $\partial v_s/\partial w$, to the change of local void ratio with time, $\partial e/\partial t$, where $e=\epsilon/(1-\epsilon)$, is given by:

$$\partial e/\partial t=-\partial\epsilon(v_L-v_S)/\partial w=\partial\epsilon v_S/\partial w \tag{7}$$

Assuming that the force balance is obtained in the whole time-space domain, i.e., neglecting the inertial effect, then:

$$p_s+p_u=p_e+w(\rho_s-\rho)g/g_c \tag{8}$$

where p_s is the solid compressive pressure, $w(\rho_s-\rho)\,g$ is related to the buoyed weight of the solid, and $1/g_c$ converts the unit to pressure.

Assuming the solid compressive pressure, p_s, and the permeability, k, are functions of solid content, then, from eqs. 3b and 7, it can be obtained that:

$$\partial e/\partial t = k\partial^2 p_u/\partial w^2 + (dk/dp_s)(\partial p_s/\partial w)(\partial p_u/\partial w) \tag{9}$$

Eq. 9 appears to be the same as obtained by Shirota et al. (1970) for systems with impervious bottom boundary. However, notice that p_u is only a component of the excess pore water pressure, and the force balance in eq. 8 involves seepage pressure. Taking the partial derivative of void ratio, i.e., $\partial e/\partial t = (de/dp_s)(\partial p_s/\partial t)$, and combining the eq. 9 yields:

$$\frac{\partial p_s}{\partial t} = K\frac{dp_s\,\partial^2 p_u}{de\;\partial w^2} + \frac{dp_s\,dk\,\partial p_s\,\partial p_u}{de\,dp_s\,\partial w\,\partial w} \tag{10}$$

Replacing the solid compressive pressure in eq. 10 results in:

$$\frac{\partial (p_u - p_e)}{\partial t} = -K\frac{dp_s\,\partial^2 p_u}{de\;\partial w^2} + \frac{dk}{de}\left(\frac{\partial p_u}{\partial w}\right)^2 - \frac{dk\partial p_u}{de\,\partial w}(\rho_s-\rho)\frac{g}{g_c} - \frac{dk\partial p_u\,\partial p_e}{de\,\partial w\,\partial w} \tag{11}$$

NUMERICAL ANALYSIS

For dimensionless numerical analysis of eq. 11, the following formula is used:

$$\frac{\partial(\phi-\psi)}{\partial T} = \frac{C_1\,\partial^2\phi}{C_1^*\,\partial z^2} + \frac{C_2}{C_1^*}\left(\frac{\partial\phi}{\partial z}\right)^2 - \frac{C_2\,\partial\phi}{C_1\,\partial z} - \frac{C_2\,\partial\phi\partial\psi}{C_1^*\,\partial z\,\partial z} \tag{12}$$

where:

$\phi = p_u/[w_0(\rho_s-\rho)g/g_c]$

$\psi = p_e/[w_0(\rho_s-\rho)g/g_c]$

$C_1 = -K\dfrac{dp_s}{de}$

$C_1^* = C_1$ at $w=w_0$ and $T=\infty$

$C_2 = \dfrac{dk}{de}w_0(\rho_s-\rho)\dfrac{g}{g_c}$

$z = w/w_0$

$T = c_1^* t/w_0^2$

and

$$\phi - \psi = z - \theta \tag{13a}$$

where:

$$\theta = p_s / [w_0(\rho_s - \rho)g/g_c] \tag{13b}$$

Experimentally the hydraulic head can be kept constant and the external resistance is usually negligible compared to the resistance of the sediment. In this case, the total pressure drop across the sediment, $\Delta P(w_0)$, is a constant; even though the applicability of eq. 11 is not limited to such conditions.

The value of dp_s/de can be found from an empirical compressive pressure vs. solid fraction relationship, which is suggested from eq. 14:

$$s = K_a p_s^{K_b} \tag{14}$$

Here s is the solid fraction defined as $s = 1 - \epsilon$, and K_a and K_b are experimental parameters. K_a represents the solid fraction at the (impervious) bottom of a fully settled ($\theta = 1$) sediment of unit buoyed weight ($w_0(\rho_s - \rho)g/g_c = 1$). K_b is related to the compressibility of the system and its value lies in between 1 and 0. When $K_b = 1$, eq. 14 resembles the ideal gas law. When $K_b = 0$, the system is incompressible, since the solid content at bottom is independent of the weight above it.

Given the particle fraction s, the permeability k can be evaluated from Kozeny's equation (Carman, 1938) as follows:

$$k = (g_c/k' S_0^2 \mu)(1-s)^3/s \tag{15}$$

where k' is Kozeny's constant, s_0 is the effective specific surface area, and μ the viscosity of fluid. The agglomerated parameter in eq. 15 can be evaluated from the initial settling velocity v_0, and the initial solid fraction s_0, according to the following equation proposed by Shirato et al. (1970):

$$(g_c/k' S_0^2 \mu) = v_0 / \{[(1-s)^3/s](\rho_s - \rho)g_c/g\} \tag{16}$$

Boundary conditions include:

$$\frac{\partial \phi}{\partial T} = 0 \qquad \text{at } z = 0 \tag{17a}$$

and

$$\frac{\partial \phi}{\partial Z} = 0 \qquad \text{at } z = 1 \tag{17b}$$

Runge-Kutta-Gill's method was used to replace eq. 12 with $(n+1)$ simultaneous finite difference equations representing the boundaries of n layers. The quantities k, dk/de, p_s, dp_s/de, $R(w)$, p_e, $\phi - \psi$ and θ can be calculated from the solid fraction s, for any time T. Applying these terms to eq. 12, a new value of θ at time $T + \Delta T$ can be found, from which a new value of s is calculated. The process is repeated successively. Therefore, the particle distribution at any

time is fully described. Consequently, the total resistance, $R(w_0)$, can be computed according to eq. 4 and eq. 15.

EXPERIMENTAL

Materials

A batch of 25%-solid kaolinite suspension (Hydrite-R from Georgia Kaolin Company) was prepared for the following experiments. The clay has a broad size distribution and 50% by weight is finer than 0.77 μm, reported by the manufacturer. The suspension has a pH 4.2.

Sedimentation measurements

The clay suspension was added to glass cylinders with cross-sectional areas of 5.16 or 3.95 cm^2, and then diluted with deionized water to desired heights. The range of the height was from 7 to 20 cm; and the solid content was from 0.1 to 2.5 g/cm^2. The suspensions were tumbled manually for 1 min at a frequency of 20 turns/min. Then the cylinders were uprighted allowing particles to settle. Sedimentation velocity was recorded for up to 7 days.

At the end of each sedimentation experiment, the supernatant and the upper part of the sediments were sucked off using a capillary vacuum tube. The rest, within 0.25 cm above the bottom of the cylinders, was sampled for solid content measurement (by overnight drying at 85°C).

Infiltration resistance measurement

The apparatus for measuring the infiltration resistance is shown in Fig. 1. About 10 g of the 25%-solid suspension was added to the soil column. The column was filled with water. The height of the water inlet and outlet were kept constant. Initially, the stopcock was closed, allowing particles to settle by their own weight on the pervious fritted glass for 24 h. The (coarse) fritted glass had an average pore diameter of 50 μm. At time zero, seepage was started by opening the stopcock. The dynamic pressure drop across the sediment and the fritted glass was measured using a pressure transducer (Celesco, model CD 10D). The eluant from the column was collected in a beaker and weighed with an electronic balance. Flow rate was computed from the differential weight of the eluant. Data acquisition and computation was carried out using a microcomputer.

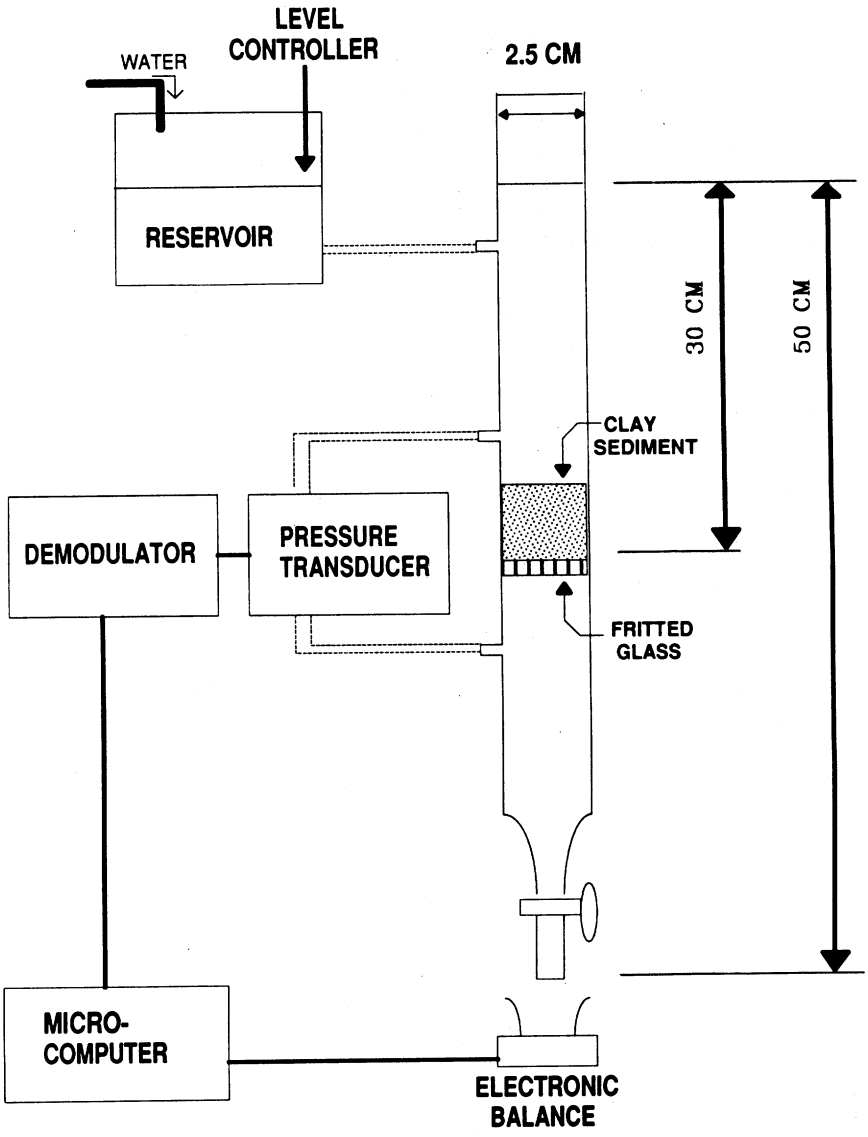

Fig. 1. Sketch of soil column.

RESULTS AND DISCUSSION

Solid compressive stress–volume fraction relationship

The clay was found to have a characteristic linear double-logarithm correlation, as suggested in eq. 14, between the compressive stress, $p_s = \text{wt} \cdot 0.6124$,

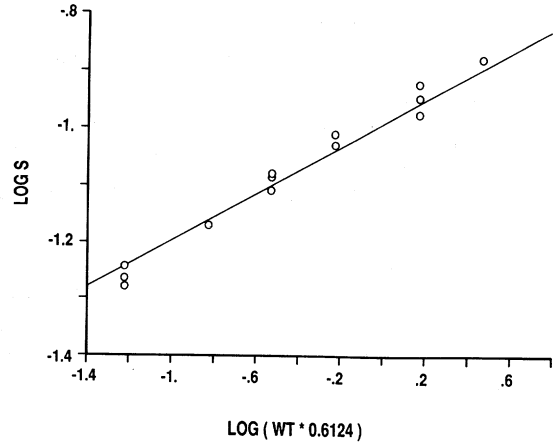

Fig. 2. Correlation between the compressive stress of solid and the solid fraction.

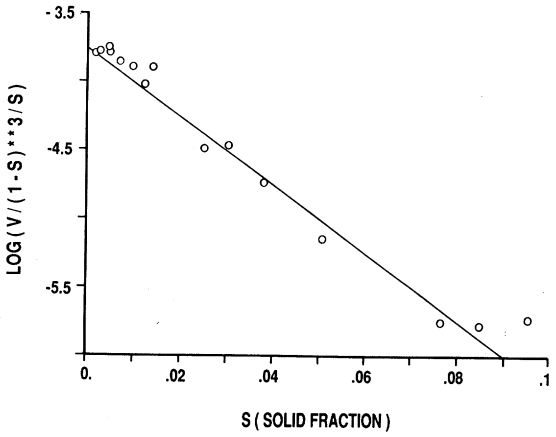

Fig. 3. Correlation between the solid fraction and the function of initial settling velocity.

and the solid volume fraction s, as shown in Fig. 2. The data plotted according to eq. 14 give 0.10031 and 0.202576, respectively, for the parameters K_a and K_b.

Settling velocity–solid volume fraction relationship

The data in Fig. 3 show a linear correlation between the initial solid volume fraction s_0, and the logarithm of $v_0/[(1-s_0)^3/s_0]$, where v_0 is the initial settling velocity. The result indicates that the suspension is non-ideal. Theoretically, for a suspension with a monodisperse particle-size distribution and an even pore size distribution, the ratio of v_0 to $(1-s_0)^3/s_0$ would be independent

of s_0, according to eq. 15. However, for flocculated suspensions, there are intra-floc and inter-floc pores. At low solid content, the size of inter-floc pores are much larger than the intra-floc pores; the settling of flocs is mostly determined by the resistance of the liquid flowing through the inter-floc pores. Therefore, S_0 in eq. 15 mainly reflects the effective surface area of the inter-floc pores. At higher solid content, on the other hand, the inter-floc pore size is reduced and liquid flowing through intra-floc channels becomes more significant. Therefore the reciprocal of the effective surface area, reflecting the ratio of $v_0/[(1-s_0)^3/s_0]$ as shown in eq. 16, decreases as the solid content of the suspension increases.

Eq. 18 was obtained from the empirical correlation shown in Fig. 3, therefore instead of eq. 15, it was used in the numerical analysis:

$$k=1.1209\cdot 10^{-4}\cdot 10^{25.039s}\cdot (1-\mathrm{s})^3/\mathrm{s} \tag{18}$$

Comparison of the theoretical and experimental sedimentation curves

Since $p_s(s)$ and $k(s)$ are obtained as described above, $\mathrm{d}p_s/\mathrm{d}e$ and $\mathrm{d}k/\mathrm{d}e$ can be computed and used in eq. 12. The equation was solved by numerical analysis with the initial suspension height, H_0, the initial solid volume fraction, s_0, and the dynamic pressure drop, $\Delta P(w_0)$ given as independent variables. The theoretical total resistance, $R(w_0)$, and the height of sediment, H, at any time during consolidation was found according to the following equations:

$$R(w_0)=\int_0^{w_0}(1/k)\mathrm{d}w \tag{19}$$

and

$$H=H_0\int_0^1(s/s_0)\mathrm{d}z \tag{20}$$

Comparison of experimental and theoretical sedimentation height-time curves of systems with clay content of 0.1, 0.25, and 1.0 g/cm^2 are given in Fig. 4, containing data at three different initial settling heights (H_0).

At low solid content, the particles settle more slowly than predicted, as shown in Fig. 4A. Experimental curves show that the settling process begins with an induction period, which may be as long as 1 min. Maximum settling velocity occurs at time=2 min. Sediment levels off at about time=4 min. Possibly, tumbling causes dispersion of particles, which may re-aggregate during the induction period to give large units with greater settling velocities. If such were the case, maximum settling velocity would not occur at the very beginning.

An induction period was found also in experiments in which the clay content was 0.25 g/cm^2, as shown by the data of Fig. 4B. However, because the sedimentation proceeds more slowly, the short induction period becomes unim-

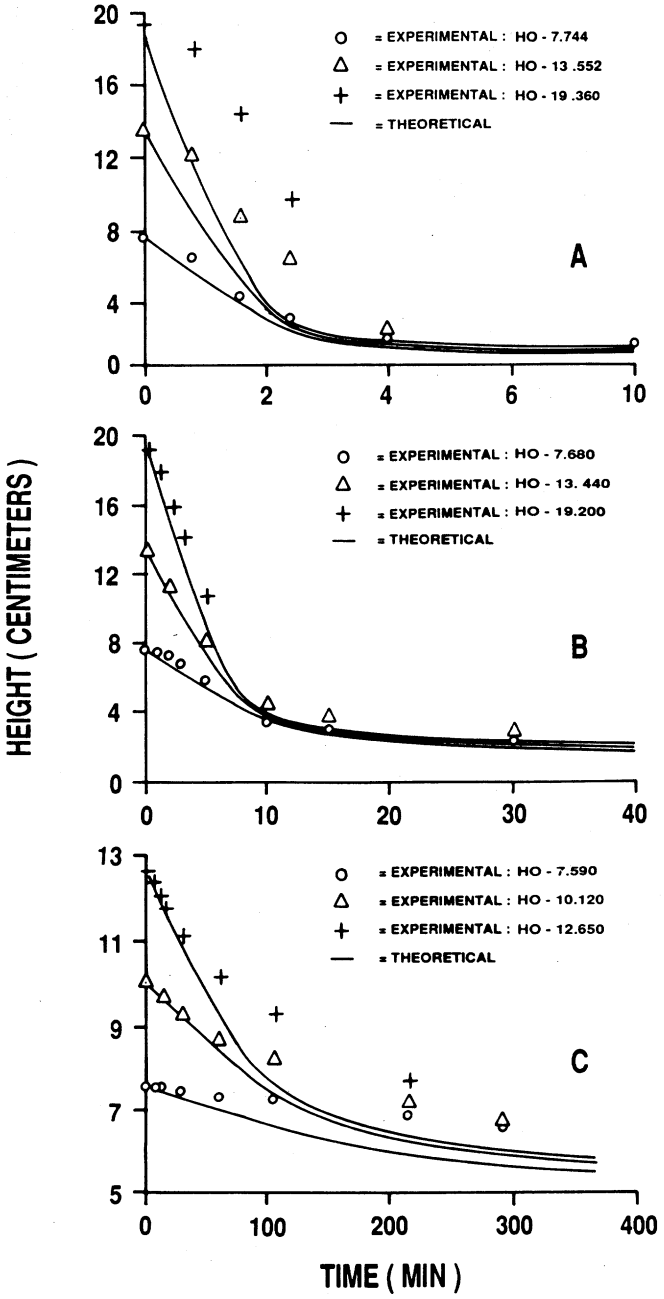

Fig. 4. Experimental and theoretical settling curves. Particle contents: A) 0.1 g/cm^2; B) 0.25 g/cm^2; C) 1.0 g/cm^2.

portant. The theoretical sedimentation curves fit the experimental data very well.

For systems with 1.0 g/cm^2 solid, in Fig. 4C, the theoretical fit of the experimental data is excellent for the first 20 min; thereafter sedimentations were slower than predicted. The discrepancy may be rationalized by postulating that the frictional force due to the cylinder wall slows down sedimentation. Frictional forces at the wall are significant only when the particle settling velocity is low. In general, the theory predicts levelling-off times quite well, regardless of how the sedimentation height is changed.

Comparison of the theoretical and experimental resistant-time curves

The pressure drop histogram of a seepage consolidation experiment is shown in Fig. 5. Pressure drop increased sharply from zero to about 50 cm water within 0.4 min after opening the stopcock and remained fairly steady thereafter.

Resistance–time data for duplicate experiments are shown in Fig. 6; data points are ○ and +, respectively. The buoyed weight of particles was 0.312 g/cm^2. The axial ratio of particles used in the experiments is unknown. Fig. 6 also shows three theoretical $R(t)$ curves obtained from numerical analysis assuming axial ratios 20, 25, and 30, respectively, for each curve; and the dynamic pressure drop was 50 cm water. Numerical analysis indicates that the infiltration resistance is very sensitive to the axial ratio of particles. It should be noted that in this article, the correlation of permeability, k, to solid fraction, s, was obtained experimentally; as was the correlation of p_s with s. By fixing the $k(s)$, dk/de, dp_s/de, the theoretical resistance curve is then determined by the axial ratio as an adjustable parameter. The figure shows that the axial ratio is inversely related to the resistance. Nevertheless, this should not be confused with

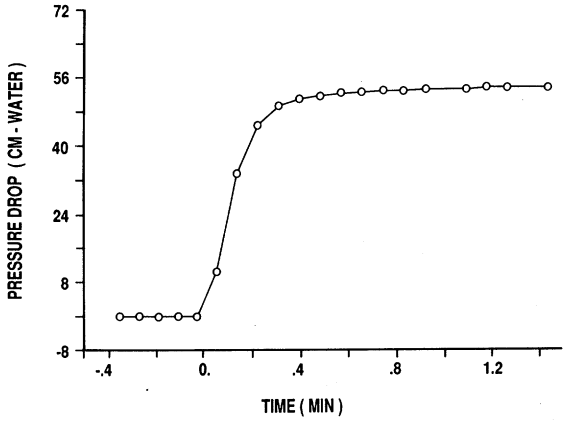

Fig. 5. Experimental dynamic pressure drop histogram.

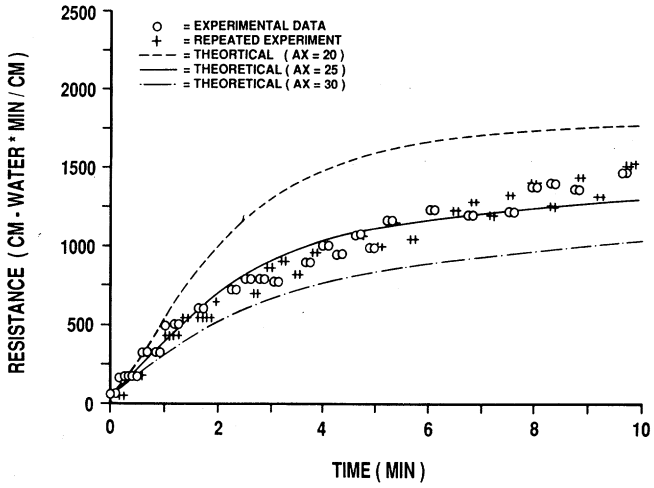

Fig. 6. Experimental and theoretical resistance curves. Buoyed weight 0.312 g/cm^2. Dynamic pressure drop 50 cm water.

the fact that systems with greater axial ratio usually give greater resistance, because axial ratio actually affects the function $k(s)$, and possibly $p_s(s)$.

Theoretical curves in Fig. 6 level off after time = 5 min, but the experimental results show that resistance is still increasing. Possibly, the discrepancy between theory and experiment is due to the wash-in mechanism. Since the size distribution of the clay particles is polydispersed, the small-size particles may remain suspended even though large particles have settled. Upon seepage, liquid carries small particles so that they penetrate into the lower region in the sediment and plug the pores down-stream where the pore is smaller than the particles. Under these circumstances, penetration may not obey the force balance principle involved in eq. 8, and deviation in theory and experiment is not surprising.

It should be noticed that our theory assumes that every particle stays in its Lagrangian coordinate during seepage consolidation. In other words, particles of the same layer must settle at the same speed, and therefore no particle can penetrate into deeper layers (i.e., no wash-in). Usually, the assumption is workable when the solid content is high, the particles are flocculated, or a gel structure forms in the system. For the systems with pH = 4.2 we noticed that essentially no particles were penetrating the fritted glass at the bottom of the sediment, even though the fritted glass has pores much larger than the particles. Apparently, the sediment behaves like a structured material and therefore our assumption is justified.

On the other hand, systems with pH $\geq$ 6.0 were different. We attempted to conduct the seepage consolidation experiment of those systems but were unsuccessful because particles penetrated through the fritted glass and therefore

the sediment can not be measured as a close system. The phenomenon indicates that a serious wash-in mechanism takes place at $pH \geq 6.0$, because particles are dispersed in the system. For those systems a different mathematical treatment is necessary to cover the transport of clay particles across laminar water streamlines by diffusion, gravity and hydrodynamic force, and the attachment–detachment of particles in glomerules due to the attraction–repulsion interaction.

Fig. 7 shows the flow rate against time curves for the experimental and theoretical systems mentioned above. In general, the theoretical curves fall in the same pattern as the experimental curves. The flow rate levels off at time = 3 min, regardless of the axial ratio. The experimental flow rate curve levels off at about the same time.

The axial ratio of the clay used in these experiments was not available. However, electron micrographs shown in the literature (van Olphen, 1977) reveal that the axial ratio of kaolinite may vary over a wide range depending on the tactoid structure of the clay. Each particle is a stack of crystalline plates. The number of plates per stack depends on the interaction of plates. The particle length in the longest dimension may be as long as 1 μm. The thickness depends on the number of plates in a stack where single plates are about 20 Å thick. The orientation of clay particles in sediments is unknown. Due to the complexity of clay sediments, the axial ratio is used only as an adjustable parameter in this article. More investigation is needed to determine if a single value of the axial ratio is applicable to seepage consolidations at various dynamic pressure drops.

It should be noted that clay sediment is non-elastic, i.e., compression is ir-

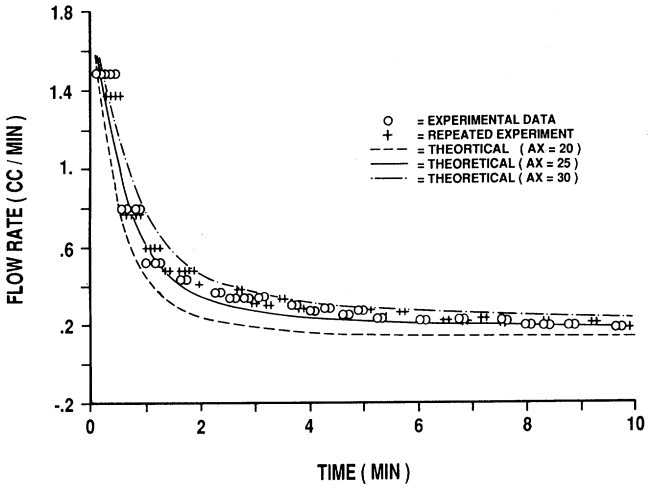

Fig. 7. Experimental and theoretical flow curves. Buoyed weight 0.312 g/cm^2. Dynamic pressure drop 50 cm water.

reversible after the stress is removed or reduced. In a seepage consolidation process, some layers in the sediment may have a compressive stress non-homotonic with respect to time. This may occur because during seepage the bottom layer always consolidates at a faster rate than other layers above. Therefore the denominator in eq. 6, $R(w_0)$, increases at a faster rate than the numerator, $R(w)$. This indicates that, unless p_u or (ϵ/τ^2) decreases at a much faster rate, p_s can be a decreasing function with respect to time. This happens particularly at high seepage pressure, as can be understood from eq. 6. Actually, a clay sediment can not expand its volume when the compressive stress decreases. To account for the non-elasticity of clay sediment, the one-to-one $s=f(p_s)$ function must be modified as follows:

$$s(t)=\max\{s(t-\Delta t), f[p_s(t)]\} \tag{21}$$

Eq. 21 indicates that the solid volume fraction, $s(t)$, at any time t is either equivalent to the previous solid volume fraction, $s(t-\Delta t)$, or correlated from the p_s-s function, which ever is greater. For the theoretical curve with axial ratio=20 shown in Fig. 6, p_s becomes non-homotonic at time=6. This is the point where the $R(t)$ curve levels off.

CONCLUSION

In this article a theory is described that uses sedimentation data to predict the water permeability of the sediment upon seepage consolidation. The infiltration resistance of sediment under seepage consolidation is a function of time, weight of solid per unit area, initial solid concentration, dynamic pressure drop across the system, and the characteristics of the sediment including the permeability, $k(s)$, the compressive stress of solid, $p_s(s)$, and tortuosity or axial ratio of the particles. In this article, $k(s)$ and $p_s(s)$ are obtained from batch sedimentation experiments. The dynamic pressure drop, the weight of solid/area, and the initial solid concentration are independent variables. When the axial ratio is 25, the theory predicts a resistance–time curve and a seepage flow rate–time curve which match the experimental curves fairly well within the first 5 min. After that, deviations occur which are believed due to the wash-in mechanism in the real system.

ACKNOWLEDGEMENTS

The author thanks Chris Beetham and Rober LaMon for their assistance in carrying out experiments and processing the data.

APPENDIX I

For a porous matrix consisting of parallel z-directional capillary tubes, the stress due to flow is related to the dynamic pressure drop, ΔP, according to:

$$P_e = \frac{n\int_0^l \int_0^{2\pi} -\mu \frac{\partial v_z}{\partial r}_{r=r_0} r_0 \, d\theta dz}{A} = \frac{n\pi r_0^2 \cdot \Delta P}{A} \tag{A1}$$

where r_0 is the radius of tube, n is the number of tubes in area A, l is the length of the system, and μ is the viscosity. Since $n\pi r_0^2/A$ is the total cross-sectional area of tubes per unit area of matrix, it is equivalent to the void fraction, ϵ. Therefore:

$$P_e = \epsilon \Delta P \tag{A2}$$

However, in a matrix with irregular pores, the flow of liquid in the x- or y-direction contributes null compressive force in the z-direction. Assuming τ is the tortuosity, the effective dynamic pressure drop applicable to z-directional channels is $\Delta P/\tau$, and the volume fraction of z-directional channels is ϵ/τ. Therefore, the compressive stress due to seepage, p_e, is approximated as:

$$P_e = (\epsilon/\tau^2)\Delta P \tag{A3}$$

The tortuosity is related to the axial ratio, L/W, according to Nielson (1967) as follows:

$$\tau = 1 + (L/W)(s/2) \tag{A4}$$

where s is the solid volume fractions, L the length and W the thickness of particles.

APPENDIX II — NOMENCLATURE

p	= excess pore water pressure (g wt./cm^2)
p_u	= a component of p (g wt./cm^2)
p_d	= a component of p (g wt./cm^2)
$\Delta P(w)$	= dynamic pressure drop from $w=0$ to w (g wt./cm^2)
$\Delta P(w_0)$	= total dynamic drop of the entire system (g wt./cm^2)
p_e	= seepage pressure (g wt./cm^2)
p_s	= solid compressive pressure (g wt./cm^2)
v_L	= velocity of liquid (cm/sec)
v_S	= velocity of solid (cm/sec)
v_F	= eluant flux (cm/sec)
w	= volume of solid per area (cm)
ϵ	= void fraction (---)
w_0	= total volume of solid per area (cm)
s	= solid fraction (---)
e	= void to solid ratio (---)
s_0	= initial solid fraction (---)
t	= time (sec)
k	= permeability (cm^4/g wt.sec)
$R(w)$	= resistance in the region from $w=0$ to w (g wt.sec/cm^3)
$R(w_0)$	= total resistance (g wt.sec/cm^3)
k'	= Kozeny's constant (---)
S_0	= effective specific surface area (1/cm)
ρ_s	= particle density (g/cm^3)
ρ	= liquid density (g/cm^3)
g	= gravitational constant (cm/sec^2)
g_c	= conversion factor (g cm/g wt.sec^2)
u	= viscosity (g/cm sec)

K_a, K_b = characteristic parameters of sediment defined in eq. 14
H = height of sediment (cm)
H_0 = initial height of sediment (cm)
τ = tortuosity (---)
L = length of particle (cm)
W = thickness of particle (cm)

t, z, C_1, C_1^*, C_2, ϕ, ψ, and θ are dimensionless, defined in eqs. 12–13.

REFERENCES

Carman, P.C., 1938. Fundamental principles of industrial filtration. Trans. Inst. Chem. Eng. London, 16: 168–188.

Gibson, R.E., England, G.L. and Hussey, M.J.L., 1967. The theory of one-dimensional consolidation of saturated clays, I. Finite non-linear consolidation of thin homogeneous layers. Geotechnique, 17: 261–273.

Gibson, R.E., Schiffman, R.L. and Cargill, K.W., 1981. The theory of one-dimensional consolidation of saturated clays, II. Finite non-linear consolidation of thick homogeneous layers. Geotechnique, 18: 280–293.

McNabb, A., 1960. A mathematical treatment of one-dimensional soil consolidation. Q. Appl. Math., 17: 337–347.

Mikasa, M., 1965. The consolidation of soft clay, a new consolidation theory and its application. Japanese Society of Civil Engineers (Reprint from Civil Engineering in Japan), pp. 21–26.

Nielson, L.E., 1967. Models for the permeability of fileed polymer systems. J. Macromol Sci., A1: 929.

Raymond, G.P., 1969. Consolidation of deep deposits of homogeneous clay. Geotechnique, 19: 478–494.

Ruth, B.F., 1946. Correlating filtration theory with industrial practice. Ind. Eng. Chem., 38: 564–571.

Schiffman, R.L. and Gibson, R.E., 1964. Consolidation of non-homogeneous clay layers. ASCE J. Soil Mech. Found. Div., 90(SM5), Proc. Paper 4043, pp. 1–30.

Shirato, M., Kato, H., Kobayashi, K. and Sakazaki, H., 1970. Analysis of settling of thick slurries due to consolidation. J. Chem. Eng. Jpn., 3: 98–104.

Terzaghi, K. and Peck, R.B., 1948. Soil Mechanics in Engineering Practice. John Wiley, New York, N.Y.

Tiller, F.M. and Shirato, M., 1960. The role of porosity in filtration, VI. New definition of filtration resistance. AIChE J., 10(1): 61–67.

van Olphen, H., 1977. An Introduction to Clay Colloid Chemistry. John Wiley, New York, N.Y., 2nd ed.

Yagi, S. and Yamazake, Y., 1960. Dewatering the compression layer in sedimentation processes. Kagaku Kogaku (Chem. Eng., Jpn.), 24: 81.